

LUND UNIVERSITY

DEPARTMENT OF GEOLOGY: RADIOCARBON GROUP

PROJECT SUBMITTED FOR THE DEGREE BACHELOR OF SCIENCE

DURATION: 2 MONTHS

Radiocarbon around the Carrington event

Author:
Damien PIERCE

Supervisors:
Raimund MUSCHELER
Florian ADOLPHI
Kristina ERIKSSON STENSTRÖM

June 2016

Contents

1	Introduction	4
2	Theory	4
2.1	Galactic cosmic rays	4
2.2	The Sun, heliosphere and modulation	4
2.3	Geomagnetic field variations	6
2.4	Atmospheric interaction and record	7
2.5	The Carrington event and "discovery" through nitrate data	9
2.6	AD774/775 event	10
3	Method	12
3.1	Tree ring sample collection	12
3.2	Precise collection for the years 1854-1864	13
3.3	Cellulose extraction	15
3.4	Graphitisation and Accelerator Mass Spectrometer measurement	16
4	Results	17
5	Data processing and discussion	18
5.1	Processing using sunspot number	21
5.2	Analysis of method	26
5.3	Further studies	26
5.4	Conclusion	26
6	References	28

Abbreviations and acronyms

- GCR: Galactic Cosmic Ray
- SEP: Solar Energetic Particle
- CME: Coronal Mass Ejection
- BABAB: Base Acid Base Acid Bleaching
- SSAMS: Single stage Accelerator Mass Spectrometer
- AGE: Automatic Graphitisation equipment

Abstract

The Sun is a volatile and complex body, understanding its behaviour is key to the continued operation of modern technology. The Carrington event was a violent white light event and generally believed to have led to one of the largest solar storms in modern human history. However the event has not been seen clearly in the ^{14}C records analysed in other publications. Here we investigate the Carrington event specifically using the cellulose extracted from tree rings. It was found that there is possible manifestation of the event in the form of an increase in $\Delta^{14}\text{C}$ of $5 \pm 2\text{‰}$ between 1859 and 1860. This is a noticeable increase but is preceded by a significant decrease for the year $\Delta^{14}\text{C}$ 1859. The reason for this decrease is unclear and could be due to errors in the experiment itself or an actual manifestation of previously unnoticed solar activity. More data would need to be collected to confirm and investigate the results found in this preliminary study.

1 Introduction

On the 1st of September 1859 a powerful solar event was observed through a telescope by Carrington (Carrington, 1859). Qualitative observations from the time confirm that this was indeed a rare event. Auroras were seen as far south as the Caribbean and sub-Saharan Africa (Odenwald 2008). This event also caused the entire telegraph system to fail (Odenwald 2002). This is why such events need to be understood, as such occurrences cause large magnetic disturbances that can destroy electronics. If it crippled the telegraph system in 1859, the damage to our orbiting telecommunications systems and ubiquitous digital equipment today could be catastrophic. An insurance report compiled by Lloyds (2013) estimated the cost of such an event today to be 0.6-2.6 trillion dollars for the US alone.

Radionuclides, such as ^{10}Be or ^{14}C can be used to improve our understanding of such events, these are isotopes that come into existence from collisions of atmospheric oxygen or nitrogen with GCR's (galactic cosmic rays) and SEP's (solar energetic particles). They are then absorbed by the biosphere or conserved in the geosphere. They form a natural record of the solar activity. Using current solar data gathered by satellites and correlating it to the natural record, we can deepen our knowledge of the sun (Beer et al, 2012). Another violent solar event that is comparable to the Carrington event was that of AD774-775 which is one of the largest in the natural archives (Mekhaldi et al, 2015) and is used as a comparison in this study.

2 Theory

2.1 Galactic cosmic rays

GCR's are assumed to be produced in supernova explosions. They consist of 87 % protons, 12 % alpha particles and 1 percent heavier nuclei (Simpson, 1983). They have been relatively constant in intensity varying within 10 percent over the past 10 million years (Wieler et al 2011). These rays travel towards us and from a distance of 150 AU are modulated by the heliosphere.

2.2 The Sun, heliosphere and modulation

Sun spots, CME's (coronal mass ejecta) and the solar wind are all different expressions of solar activity. Sunspots are regions of highly varying magnetic fields of up to 3000G (Beer et al, 2012). There is an 11 year periodicity in

sunspot number and a 22 year periodicity within uncertainty in the polarity of the solar magnetic field (Beer et al, 2012). The corona is a region of gas that surrounds the sun. High coronal temperatures lead to gas streaming out, called the solar wind. It has very low electrical conductivity and thus freezes in the solar magnetic field within itself (Beer et al,2012). The solar wind propagates out in a spiral (Parker 1958,1963).

In times of higher solar activity, the number of sunspots increases, this can lead to magnetic disturbances, causing rapid magnetic heating of the gas and ejection of the produced plasma at high velocity i.e to a CME . Solar flares are an intense brightening of the area around a sunspot leading to a large release of energy.(Beer et al,2012).

Solar energetic particles are usually much lower in energy than GCR's but can cause peaks in radionuclide production(Lal and Peters 1967), if the event was energetic enough. The solar magnetic field interacts with GCR's outside the immediate area of the sun. A numerical cosmic ray propagation equation can be used to calculate the path of cosmic rays through the heliosphere but it is very complex. Most often a quasi empirical formula called the modulation function is applied as an approximation of the attenuation of a cosmic ray dependent on kinetic energy (Beer et al 2012). Most of the cosmic rays that reach the top of atmosphere have more than 20 MeV in energy. Figure 1 shows the flux of cosmic rays and their modulation at the top of earth's atmosphere

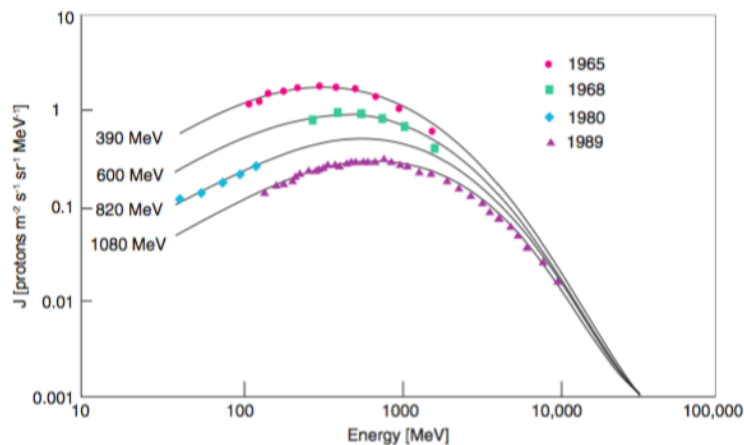


Figure 1: Flux of cosmic rays dependent on energy. Best fit lines from data gathered by high altitude balloons in 1965,1968, 1980, 1989, after Bonino et al (2001)

2.3 Geomagnetic field variations

Convection currents within the earth cause the earth to have a magnetic field. The magnetic field of the earth, although complex, can be approximated to a dipole. There is very little modulation of the cosmic ray spectra around the poles with the current geomagnetic scheme. The flux of cosmic rays increases by a factor of two at more northern latitudes compared to the equator (Beer et al 2012). The geomagnetic cut off rigidity must thus be taken into account. It is an equation that takes into account momentum and charge per nucleon and integrated flux to determine the intensity of the incoming cosmic ray. The results imply that at the equator the cut of rigidity is 14 GeV for protons and 6.5 GeV per nucleon for helium. This decreases with latitude (Beer et al 2012). A plot taken from Beer et al (2012) is presented in figure 2 and shows the variation of cut off rigidity with latitude. It is evident that cosmic rays that are incident at a higher latitude are modulated to a much lower degree than those at the equator. As can be seen in the figure angle of incidence is also an important factor in determining the cut off rigidity.

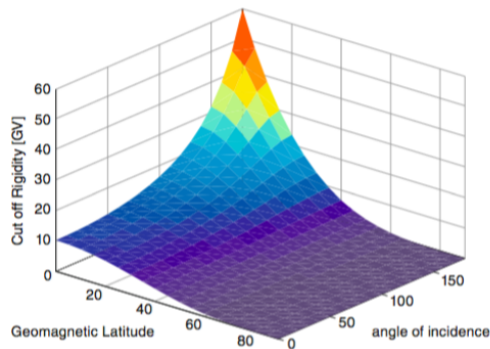


Figure 2: Geomagnetic cut off rigidity for cosmic rays dependent on angle of incidence and latitude from Beer et al (2010)

The geomagnetic field shows evidence of long term non-periodic variation. Figure 3 shows an approximation as a colour map of the geomagnetic field at the core mantle boundary for the year 1890 from Jackson et al (2000). Blue shades represent flux into the core, red shades are flux out of the core.

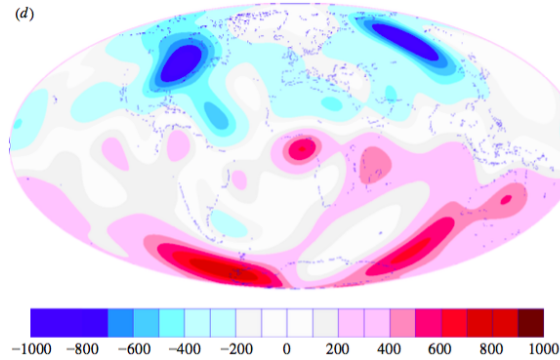


Figure 3: The radial field at the core mantle boundary on an equal-area projection. The contour interval is $100 \mu\text{T}$. Blue shades represent flux into the core, red shades are flux out of the core.

2.4 Atmospheric interaction and record

Radiocarbon (^{14}C) is mainly produced from atmospheric nitrogen and oxygen. The binding energy per nucleon is high for these elements, thus ^{14}C is not created spontaneously (Beer et al 2012). Incoming particles will create reaction products, and some of these will decay/produce other particles. The Bethe-Bloch equation applies here and can be used to compute energy loss, as incoming rays and produced nuclides lose energy mainly through ionisation (Beer et al, 2010). The production rate of nuclides in the atmosphere has been derived by complex computer codes such as the research done by Masarik and Beer (1999).

In the Masarik/Beer experiment, the atmosphere was approximated to 34 shells each much smaller than the average mean free path of the particles. To account for the geomagnetic cut off rigidity 9 bands were created so that the rigidity would be approximately the same in each band. The production of nuclides was also calculated considering the solar modulation and the effects from the geomagnetic field.

Radionuclides are mainly produced in the the stratosphere and the troposphere, as the air density is so low above the stratosphere that few radionuclides are produced above it. Atmospheric circulation is a key element in understanding radionuclides since it is responsible for the global mixing.

From the earths rotation and temperature differences, convection cells are formed, which transport and mix the air. This temperature difference also causes the air to rise, and as it rises, it cools at the "lapse rate". The barrier between the troposphere and stratosphere is called the tropopause

and defined as the region where the lapse rate is lower than $2Kkm^{-1}$, it is strongly latitude dependent due to uneven power delivered by the sun at different latitudes. In the stratosphere a strong stratification is present due to the fact temperature increases with height, thus residence times are longer in the stratosphere.

When ^{14}C is formed it first becomes $^{14}CO_2$ based carbon dioxide and it remains in the atmosphere for approximately 7 years if well mixed. The signal recorded in archives is therefore smoother and is more indicative of global averages (Beer et al, 2012). The CO_2 is partly absorbed by plants, and living creatures as part of the carbon cycle. Most carbon in the atmosphere dissolves itself in the ocean and is incorporated into sediments that then subduct and are recycled through volcanic eruptions (Oeschger et al, 1975). Figure 4, from Sturm and Lotter (1995), shows a schematic of this process.

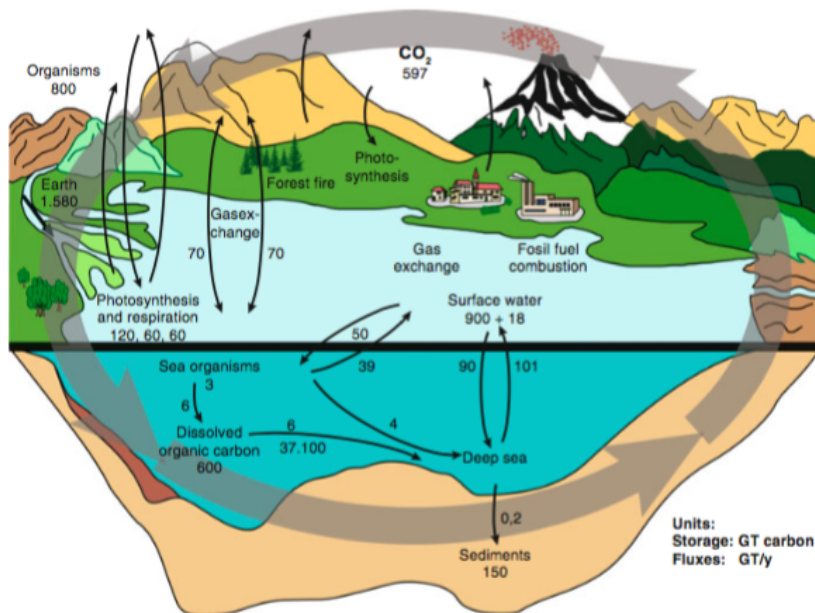


Figure 4: The carbon cycle in GT, with the numbers at the arrows showing flux in GT per year, from Sturm and Lotter (1995)

A box diffusion model can be used to model the cycle quantitatively. If the ^{14}C production rate is modeled as a sinusoidal function. It mirrors the 11 year solar variation, but the system does not linearly reflect a change in ^{14}C . It is out of phase by 1/4 of a solar cycle (Stuiver et al, 1993).

2.5 The Carrington event and "discovery" through nitrate data

The event observed by Carrington is described as follows in his paper,

"In the forenoon of Thursday September 1[...]two patches of intensely bright light broke out in the positions on the appended diagram at A and B (see figure 5)[...]returning within 60 seconds[...]it had much changed and enfeebled[...]the last traces were at C and D [...]the instant of the first outburst was not 15 seconds different from 11h 18m Greenwich mean time, and 11h 23min taken as the time of disappearance."(Carrington, 1859). The ensuing storm had a very short travel time of 17.1 hours (Cliver et al 1990). This was accompanied by what is called a geomagnetic crochet, an extreme X-ray and ultraviolet light event. The photons that are then absorbed in the ionosphere cause further ionisation leading to a large current flow in the earth's magnetic field (McCracken et al, 2001).

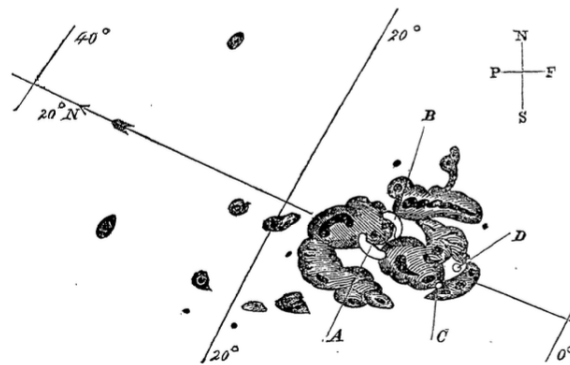


Figure 5: Drawing made by Carrington during the Observation of the solar event (1859) showing the movement of the sunspot from points A,B to C,D

The fluence (number of particles over a certain energy incident per cm^2) of the Carrington event was determined through the nitrate data by McCracken et al (2001). Nitrate is present in ice as a result of "odd" nitrogen, of the form NO_y (NO, NO₂ etc) produced by energetic particles. The quick succession of snowfalls and their subsequent compaction to what is called firn creates a natural record with a high temporal resolution. The individual layers were dated using layer counting. Correlation functions along with a model for deposition were used in accordance with the data gathered by accurate modern records from satellites to determine the fluence of previous events. McCracken et al (2001) determined the Carrington event to have a fluence at $> 30MeV$ of $18.8 * 10^9 cm^2$. They also determined it to be the highest peak in nitrates in their entire data set spanning 1561-1994. This is

an exceptionally large event and is close to a practical maximum for SEP's, due to the streaming limit.(see below)

As SEP's increase in fluence, the interactions between themselves increase, and thus above a certain energy they are unable to escape the heliosphere. This is called the streaming limit (Reames 1999). It is however arguable that the nitrate data is wrong, as the Carrington event is not seen in any other publications, such as Stuiver et al (1993) and Usoskin et al (2006)

2.6 AD774/775 event

Another massive solar eruption has been found to have occurred in AD774/775. A correlation between ^{10}Be , ^{36}Cl and ^{14}C was done by Mekhaldi et al (2015). built on the work of Miyake et al (2012). It was found using $\Delta^{14}\text{C}$ and the ^{14}C production rate that the fluence of this event was $> 30\text{MeV}$ of $2.8 * 10^{10}\text{cm}^2$. There is a clear peak in the data for all three radionuclides, a graph of their findings is presented in figure 6. The ^{14}C production rate was calculated from $\Delta^{14}\text{C}$ in Miyake et al (2012). In the Miyake paper, samples from 2 cedar trees were taken between the years 770 and 779, and the $\Delta\text{C}14$ was found experimentally. A peak was found around AD 774/775, with this in mind, disregarding energy differences,it is reasonable to expect to find a peak for the Carrington event of some magnitude. Usoskin et al (2006) found that the Carrington event did not appear in the ^{14}Be data from NGRIP or the DYE3 records.

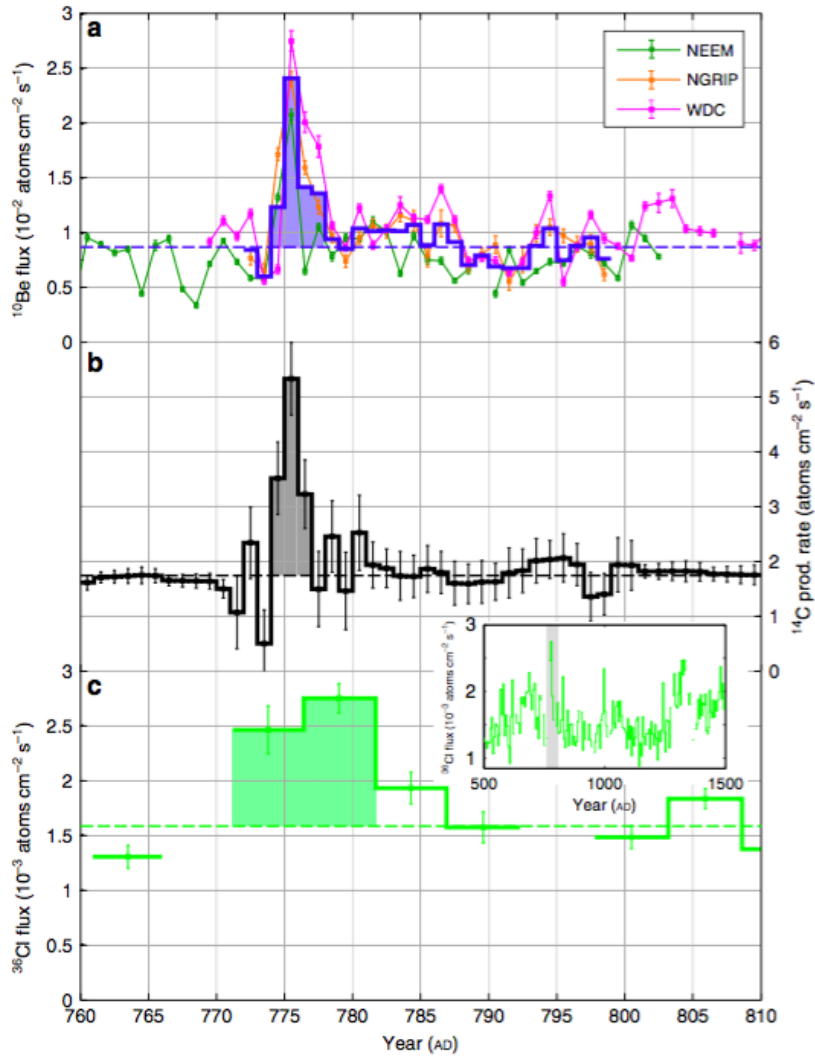


Figure 6: Graphs of the peaks in radionuclide flux found by Mekhaldi et al (2009) in ^{10}Be , ^{36}Cl from two ice drilling stations in Greenland and ^{14}C production rate calculated using $\Delta^{14}\text{C}$ from Miyake et al(2012)

The Carrington event thus only appears in the highly debated nitrate data. All of the other radionuclide records arguably do not show any evidence of a strong solar event in 1859. Yet the damage to our orbiting satellites would be catastrophic if the same event were to manifest itself today (Lloyds, 2013). An in depth look at the radiocarbon record for the particular set of years surrounding the Carrington event is thus useful to see if a more detailed study would indeed reveal evidence of the event and allow us to improve our understanding of the radiocarbon record and thus solar

activity.

3 Method

I prepared graphite samples from tree rings that grew around the period of the Carrington event. The graphite was then analysed for its ^{14}C content with the single stage accelerator mass spectrometer (SSAMS) at Lund University. A detailed account follows.

3.1 Tree ring sample collection

The tree in question that was used for this study is piece of an oak tree that was cut down in 1998 and was a sapling in the late 17th century. The tree was located on the border between the Swedish province of Blekinge and Småland. A small piece of this tree, around the target years, was the focus of collection. Figure 7 shows a picture of the sample with the tree rings of interest marked on with their year of growth. These dates were determined by the dendrochronology laboratory in the Geology department at Lund University prior to the start of the experiment.

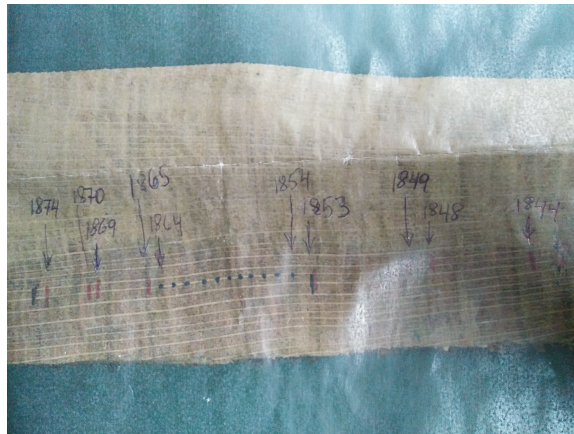


Figure 7: Tree rings of interest and their annual layers before sample collection began (growth direction is to the left)

A device using a sharp razor blade was used for the sampling. The objective was to collect 4 year averages across the rings for the years 1870-1874, 1744-1858, 1865-1869, 1849-1853. This was done to the highest qualitative degree of precision. It was difficult to get clear uniform pieces.

The years of high interest, 1854-1864 were collected with a different method. A cut was first made of all the tree rings from those years and then split into 3 pieces to allow for resampling if necessary. The more precise method had the drawback of destroying the sample as data was collected, as opposed to carefully shaving off the top which would have allowed much more wood to be collected if necessary.

3.2 Precise collection for the years 1854-1864

Each of the samples within these years corresponded to individual tree rings. It would be impractical to attempt to shave across the rings. Figure 8 shows a picture of an individual block of years.



Figure 8: Tree rings of interest before sample collection began

As can be seen in figure 9, the advantage of cutting the block up in this fashion is that it exposes an entire tree ring along the depth of the block, allowing precise determination of which year is being sampled. The figure also shows the structure of an individual tree ring, there are darker bands and lighter bands. The lighter part of the rings grows first and contains larger vessels, the harder darker part grows after, and has smaller vessels.

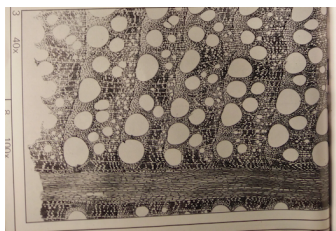


Figure 9: Drawing of the microscopic structure of oak tree rings from Schweingruber (2012)

The lighter part with the large veins is known to be less dense but contains more cellulose, whereas the darker part with the smaller veins has a lower cellulose content, but is denser.

The razor blade was first used to shave off individual samples from the ring. The ring itself was then wittled down until none of the previous ring remained. A new sample was taken halfway through the next darker band. To be sure there was nothing remaining of the previous ring, a microscope was used to determine this exactly. A picture in figure 10 shows how the microscope was used to determine which tree ring was being collected.

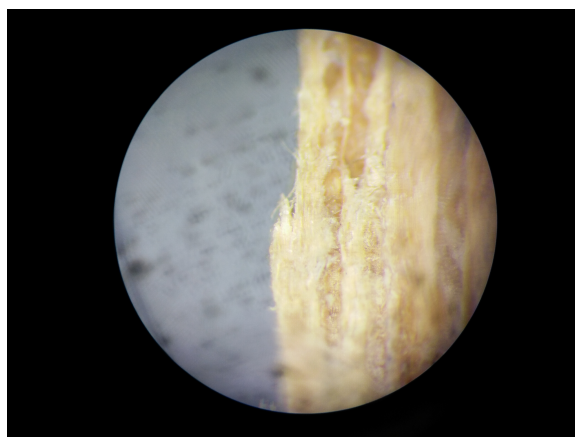


Figure 10: The microscopic structure of oak tree rings

In the picture it can clearly be seen there is no remnant of the darker ring of the previous year.

All the samples were collected in such a way that they were approximately the same size and thickness, which is key for the cellulose extraction as all pieces will reduce at the same rate.

3.3 Cellulose extraction

The cellulose extraction is a chemical process. Cellulose is present in a crystalline form in the cell walls and is a linear polymer (Nemec et al 2015). The BABAB (base, acid, base, acid, bleaching) was used. The samples were first soaked in 4% NaOH overnight at 75 degrees. they were then washed by pipetting out the solution and filling the beaker with ultra pure distilled water, and emptying, 5 times. The beakers were filled with 4 % HCl, and placed in the oven for a further hour, and then washed again. This process was repeated twice (Nemec et al 2015). The aim of the BABA steps is to fragment the lignin network to simplify the cellulose extraction (Nemec et al 2015). The Samples were then placed in a water bath at 85 degrees with a solution of 4% $NaClO_2$. This step required a qualitative judgement of whether the cellulose extraction is complete. The samples were not reduced to pure cellulose, as that would reduce the yield, the cellulose was extracted to a degree that was deemed an acceptable compromise between quality of cellulose and ease of extraction. Figure 11 shows a sample right before the final washing.



Figure 11: Qualitative representation of the degree to which the cellulose was extracted (white strands are the cellulose)

After this process, the samples were washed a final 5 times, placed in a vial, weighed with an analytical balance and dried overnight.

The beakers used were duran glass beakers and were cleaned in the following way, rinsed with tap water, soaked in 4% $NaOH$ overnight, rinsed again, soaked in HNO_3 overnight, rinsed one last time, soaked in distilled water overnight, rinsed with ultra pure distilled water and finally dried overnight in an oven.

Precautions were taken to prevent contamination. Any surfaces the beakers touched were extensively cleaned with ethanol, and aluminum foil was placed as a cover at all times. The beakers were always covered with tops. Each pipette was only used for one beaker and discarded if it touched a waste beaker, or any other possibly contaminated surface. Washed beakers were placed in the cupboard covered in aluminum foil to prevent contamination. gloves were worn at all times.

3.4 Graphitisation and Accelerator Mass Spectrometer measurement

The Graphitisation was performed following the methodology as described in detail in Wacker et al (2012). Samples of 3,8 to 4,2*mg* of cellulose was first weighed in to small tin capsules and then folded carefully with tweezers into a small ball. 2,8 to 3,2*mg* of pure iron powder was then weighed into small glass tubes. The samples were placed in the AGE (automatic graphitisation equipment) and graphitised (Wacker et al, 2010).

The samples are manually pressed into flat discs and placed into an accelerator mass spectrometer wheel and were measured at the single stage accelerator mass spectrometer (SSAMS) at Lund University as described in detail in Skog et al (2010).

4 Results

Presented in Table 1 is the raw data gathered from the AMS, the sample ID's are named according to the professional radiocarbon laboratory naming system at Lund University. The radiocarbon age was automatically calculated at the time of measurement using the equations described in detail in Eriksson et al (2011).

Table 1: Table of raw data from AMS, samples 201.8.1 and 201.9.1 are the known samples (BP: before present)

Sample ID	Age (years) from ring counts	Radiocarbon age (years BP)	σ (years BP)
201.8.1	5067-5075	6187	28
201.9.1	5067-5075	6235	31
606.1.1	1856	142	22
606.1.2	1856	143	22
607.1.1	1862	173	23
607.1.2	1862	133	22
607.1.3	1862	140	22
608.1.1	1863	148	22
608.1.2	1863	145	24
608.1.3	1863	122	22
609.1.1	1864	127	24
609.1.2	1864	144	22
609.1.3	1864	157	23
610.1.1	1857	129	23
610.1.2	1857	125	23
610.1.3	1857	132	23
611.1.1	1858	93	22
611.1.2	1858	108	23
611.1.3	1858	113	23
612.1.1	1859	187	22
612.1.2	1859	166	22
612.1.3	1859	179	27
613.1.1	1860	148	22
613.1.2	1860	140	22
613.1.3	1860	104	23
614.1.1	1861	158	23
614.1.2	1861	107	24
614.1.3	1861	162	23

5 Data processing and discussion

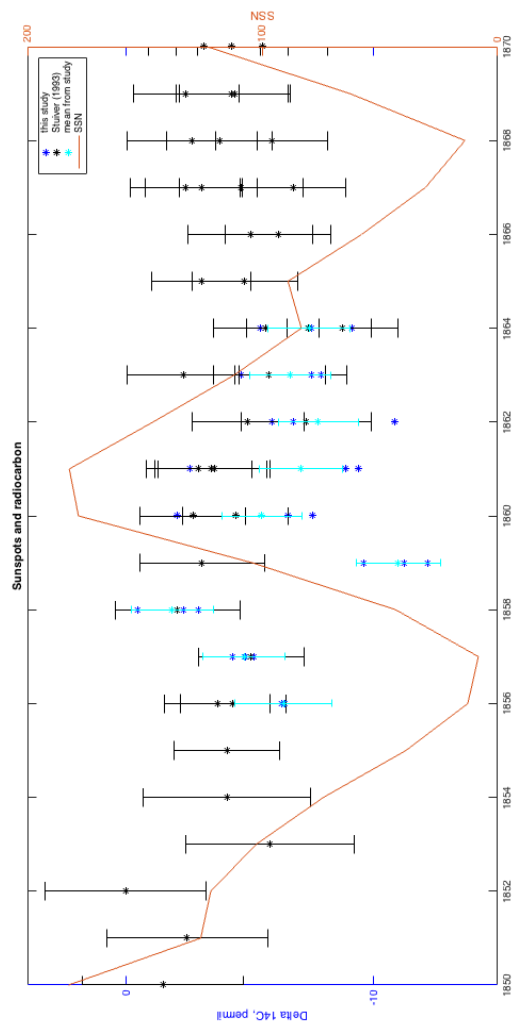
Data processing and a general discussion of how the data from this study compares to the data based on Stuiver(1993). This is a data set that is considered a good standard for comparison for $\Delta^{14}C$ for the past 500 years.

The quantitative treatment of ^{14}C was done as follows. The measured quantity was the age of the sample in calendar age BP (before present), which is equivalent to the ^{14}C age of the sample. These ages were then compared to an industry standard and a blank sample, in the form of old wood with no ^{14}C left used for assessing the quality of the data. A thorough overview of the mathematics behind this along with descriptions of the standards is available in Eriksson et al (2011). From the age in calendar years BP, the ratio $^{14}C/^{12}C$ known as $\Delta^{14}C$ can be computed using equation 1. $T_{^{14}C-years}$ is the age in calendar years BP. $T_{cal-years}$ is the year 1950 subtracted from age deduced using dendrochronology.

The data is presented in Figure 12 as $\Delta^{14}C$ of the error weighted mean of all the measurements in calendar years BP. The results have been graphed with the average yearly sunspot numbers from SILSO (Royal Observatory of Belgium, Brussels) to observe how the data compares to sunspot numbers. and the data previously measured by Stuiver et al (1993).

$$\Delta^{14}C = e^{-\frac{T_{^{14}C-years}}{8033}} \cdot e^{\frac{T_{cal-years}}{8267}} \cdot 1000 \quad (1)$$

Figure 12 is presented on the next page in landscape for clarity



45

Figure 12: Graph of the $\Delta^{14}C$ with the data from Stuiver (1993) and yearly sunspot number

The data collected in this study lies qualitatively within the uncertainty bars of the Stuiver data, indicating a good agreement, as can be seen in Figure 12. The highest quantitative disagreement is for the point 1859 of $7 \pm 3\%$. A reduced χ^2 test was then performed, comparing the Stuiver data and the data collected in this study, this yielded a value of 2.1935.

A quantitative comparison with the Stuiver data was performed using equation 2. $\Delta^{14}C_O$ is the $\Delta^{14}C$ calculated in this study, $\Delta^{14}C_S$ is the $\Delta^{14}C$ calculated from the Stuiver paper, δ_O and δ_S are the uncertainties in $\Delta^{14}C$ for each study respectively.

$$diff = \Delta^{14}C_O - \Delta^{14}C_S \pm \sqrt{(\delta_O)^2 + (\delta_S)^2} \quad (2)$$

An error weighted mean was found from the resulting vector, this is the average quantitative difference in $\Delta^{14}C$ between this study and the Stuiver data from 1993. This average is then added to the data from this study to study how the data sets agree. The resulting plot is presented in Figure 13, where the points have been shifted upwards by $1.9 \pm 0.9\%$

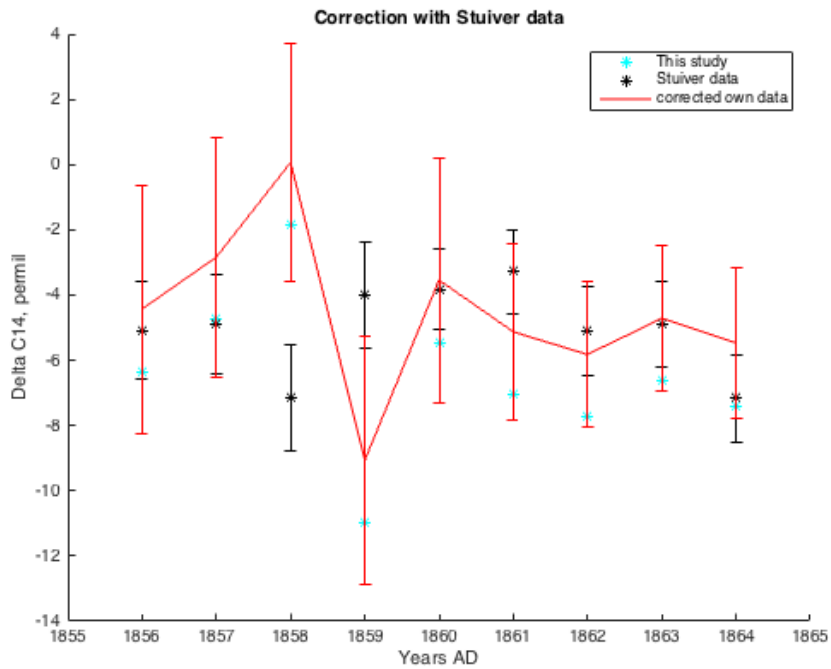


Figure 13: Correction using quantitative difference between Stuiver data (1993) and own data

In Figure 13, compared to the raw unprocessed data, the amplitude variation between the points is lower and the point for 1859 has been shifted up. The point for 1859 even with correction shows a sharp decrease in $\Delta^{14}C$ followed by a sharp increase for 1860, reflecting the original data from this study. It can be calculated that the point for 1859 is in disagreement of 368 percent of the average disagreement between the two sets, which is nearly 4 times the average difference.

5.1 Processing using sunspot number

The next step is attempting to eliminate the 11 year inverse relation between sunspot number and $\Delta^{14}C$ to determine whether the peak produced is indicative of unusual solar activity, or just a manifestation of regular solar variation. In the Stuiver paper (1993), the $\Delta^{14}C$ was modeled as a periodic function in relation to solar activity in the form of sunspot numbers. It was found that the peak to trough difference in $\Delta^{14}C$ was 2.8‰ if only solar activity variation is considered. It was also found that the ^{14}C production rate is out of phase with the sunspot data by a quarter of solar cycle (i.e it is the time required for changes in production rate to manifest themselves in the ^{14}C data).

Thus, removing the variation due to solar activity requires shifting the points up or down depending on the solar activity at the time. The $\Delta^{14}C$ in times of highest solar activity would be shifted up by 1.4‰, whereas the $\Delta^{14}C$ in times of lowest solar activity would be shifted down by 1.4‰. A complication arises for determining the amount of correction that needs to be applied to any point that is neither a maximum or a minimum. For this a function needs to be found, the procedure is described below.

The sunspot data from 1700 to 1950 was sorted in ascending sunspot number. The resulting vector was then plotted against a linear vector of 250 points that were equally spaced from $-1.4‰$ to $1.4‰$. These sets of points were then fitted to find a function that described its behaviour, using MATLAB's inbuilt `cftool`. A linear fit was deemed too rough, with an R^2 value of 0.9259. An 8th degree polynomial fit was used instead with an R^2 value of 0.9987, this could present a risk of going to infinity very quickly at large sunspot values. The increase in precision however justifies the use of such a function. This function was used to find the magnitude for which each point needed to be shifted.

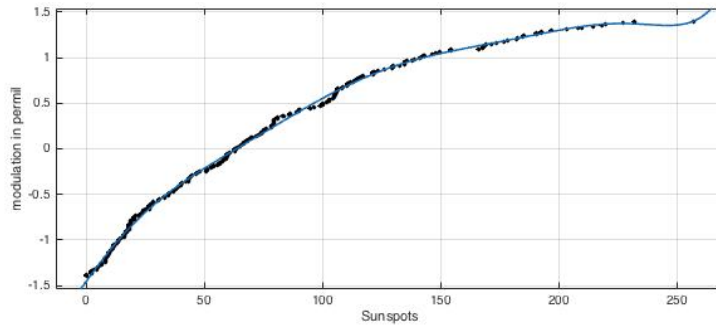


Figure 14: Graph of yearly sunspots in order of ascending sunspot number against a linear space from -1.4‰ to 1.4‰ representing an estimated $\Delta^{14}\text{C}$ change with solar activity. Fitted with an 8th degree polynomial (blue line)

This processing method produces the following smoothing to the collected $\Delta^{14}\text{C}$ data.

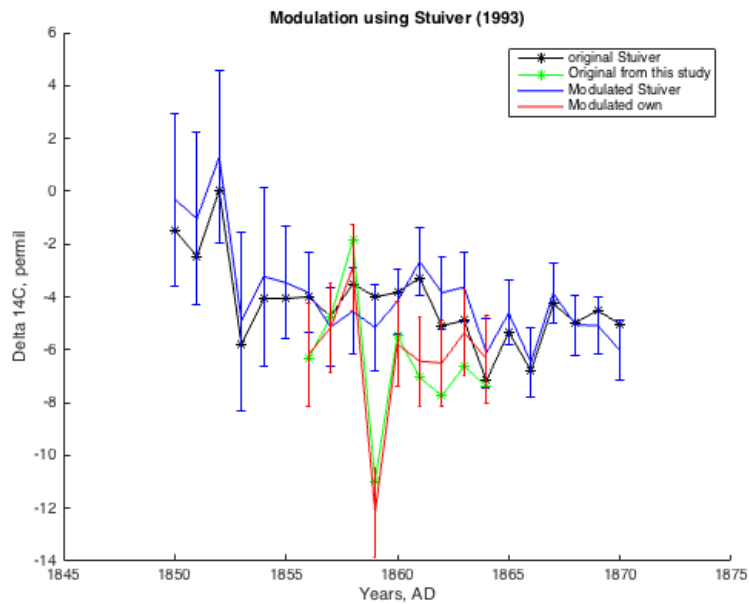


Figure 15: Smoothing using the function above to correct for sunspot variation according to findings concerning solar variability effects on ^{14}C production rates from Stuiver(1993)

By applying the same processing method using equation 2, an average difference between the Stuiver data and this study for 1859 of 1.19‰

was obtained. The peak in the year 1859 is still plainly visible, and only shows a slight attenuation.

In an attempt to try and reduce the effect from solar variation using a different method, a low pass filter was applied using the inbuilt MATLAB low pass filter function. The results are presented in figure 16.

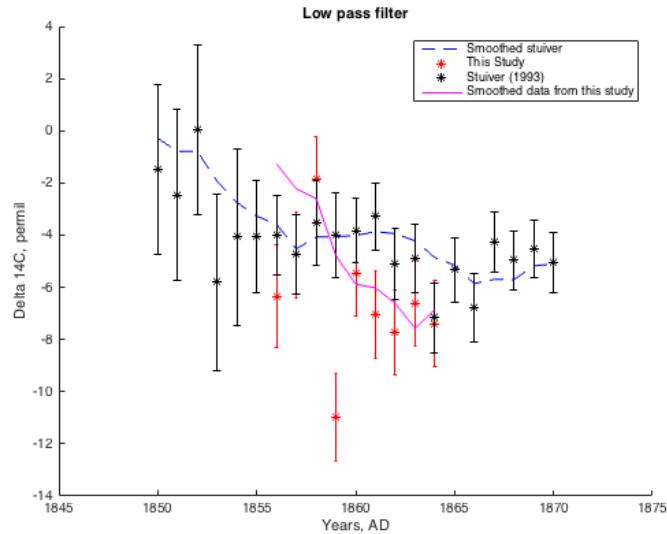


Figure 16: Low pass filter using inbuilt MATLAB function *filter*

In figure 16, a clear smoothing of both functions is visible. The sharp gradient between 1858 and 1859 suggest that after filtration the effects of the 1859 point are still significant, albeit attenuated. The low pass filters are qualitatively more effective for the Stuiver data due to the increased amount of data available for processing. A wave like undulation is still present suggesting the solar modulation has not been completely removed, assuming that solar activity is the only factor affecting the Stuiver data. Attempts were made to smooth the data to a higher degree by using smoother filters, these however lead to a complete attenuation of both curves and the disappearance of any features in both.

The behaviour observed for the 1859 point in figures 13,15 and 16 is indicative of a decrease in $\Delta^{14}C$, an unexpected feature. The difference between the point for 1859 and 1860 is $5 \pm 2\%$, a significant increase, suggesting that in absolute terms there is possible evidence for the Carrington event. Looking at Miyake et al (2012) for the more powerful AD 774/775 gives a change of 8% from an observation of their results (figure 17). Considering the differences in fluences, it can be argued that this sharp change in the

data from this study between the years 1859 and 1860 is indicative of the Carrington event, as in terms of absolute difference in $\Delta^{14}C$, the increase observed is important, yet less than that of the AD 774/775 event. This is assuming our data is correct, as this feature is absent from the Stuiver data.

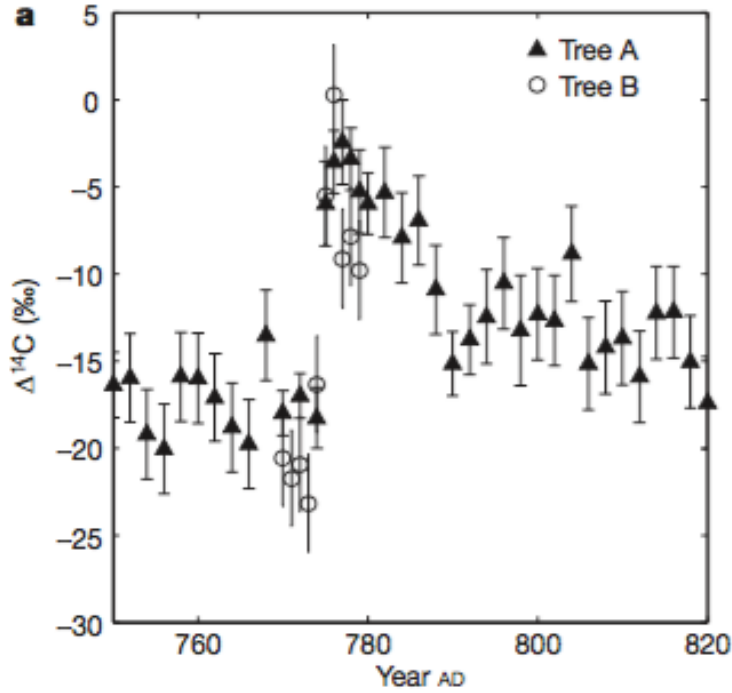


Figure 17: Data from Miyake et al (2012), showing decadal changes in $\Delta^{14}C$ (presented here for completeness with no further processing)

Contamination of the sample is also a possibility for the point 1859. If we postulate that the point should have the same magnitude as the equivalent point in the Stuiver data, this would mean the point needs to be shifted upwards by a factor of $7 \pm 3\%$. Two possibilities arise. A contamination from dead wood, i.e from old samples that contain no ^{14}C , rearranging equation 1 and evaluating to solve for $T_{14C-years}$ with $\Delta^{14}C$ as 7 in MATLAB, we thus obtain the order of magnitude in calendar years BP needed to offset the data by $7 \pm 3\%$. We can determine using simple calculation that the fraction of cellulose required needed would be 0.05 percent of the sample. Assuming a 5 percent yield of cellulose and a $3.2mg$ sample gives a contamination of $3.2mg$ of actual unprocessed wood for a $25mg$ sample, which clearly improbable. For "modern carbon". It is highly unlikely that it would cause a significant error, as there would need to be a higher degree of contamination as the modern wood has a similar $\Delta^{14}C$ as the tree rings

around 1859. Thus contamination is improbable, considering the method used to extract the wood from the tree rings. Furthermore it is unlikely that the 1859 sample would be contaminated to such a degree and none of the others.

Looking at the reduced χ square values from this study and comparing them to the findings by Adolphi et al (2013), it can be concluded that the differences between the 2 data sets when the 1859 point is disregarded, lie within the reduced χ square values that arise from differences in laboratory preparation techniques for identical samples, suggesting that any difference arising between the data sets can be attributed to the expected variation between laboratories.

The Stuiver data set from 1993 was updated in 1998, the differences between the two are investigated. In figure 18.

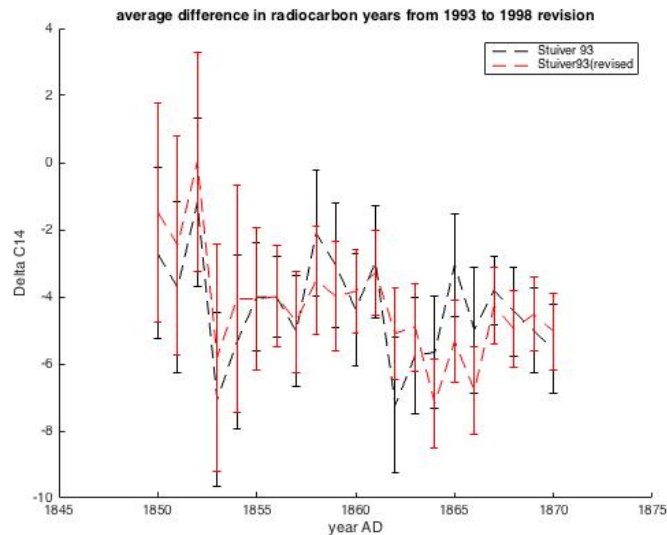


Figure 18: Differences $\Delta^{14}C$ in ‰ from 1993 to 1998 for Stuiver data

Looking at the difference between the two Stuiver sets quantitatively, an average disagreement was obtained of $-0.15\text{‰} \pm 0.4\text{‰}$, hence the disagreement between the two data sets is negligible. Furthermore the difference for the point 1859 is $1\text{‰} \pm 2\text{‰}$, also negligible.

5.2 Analysis of method

The main drawback of the methodology is the way the raw samples were collected. It was difficult for an inexperienced person to collect good wood samples using the tools provided. It was also difficult to see the actual tree rings even under the microscope and their undulation and unpredictable thicknesses often resulted in confusion and meticulous rechecking was necessary. Some way of splitting the wood more precisely along the tree rings before collection began would improve precision. A more precise collection tool that is easier to hold and use would also improve the quality of the raw data. The pieces collected were all very thin which meant they disintegrated very easily when it came to cellulose extraction and therefore resulted in a lower yield.

The chemical cellulose extraction was tedious and a large amount of cellulose was lost due to very delicate fibers being pipetted out during the washing process. Possible contamination could have been caused when the beakers were in the water bath as the air escaping from the bath itself caused the beakers to rattle around and knock into each other. Every time a glass top was removed to check on the dissolution the chances of contamination was increased.

5.3 Further studies

It would be worthwhile to compare the data from this study to an identical set from the same tree but prepared by the professional carbon lab, to investigate the possibility of human error. Re-sampling for 1859 would also be a good suggestion for further analysis as would sampling individual tree rings for the entire set 1850 to 1870, and using the same processing techniques, to improve the efficiency of the low pass filter by providing more data.

5.4 Conclusion

From the data collected, and the data processing, some conclusions can be drawn. The sharp decrease in 1859 followed by a sharp increase for 1860 does suggest a possible event, yet there is no conclusive explanation for the decrease. With filtration it can be seen that the Stuiver data and the set from this study mirror each other, and along with chi square tests, suggests that these sets agree, except for the point for 1859. More data would need to be collected to determine whether this point is an outlier. Yet it is possible

to say that the behaviour observed in this study is unique, further studies remain to be done to determine whether any meaningful conclusions can be drawn.

6 References

- Adolphi, F., Güttler, D., Wacker, L., Skog, G. and Muscheler, R., 2013. INTERCOMPARISON OF ^{14}C DATING OF WOOD SAMPLES AT LUND UNIVERSITY AND ETH-ZURICH AMS FACILITIES: EXTRACTION, GRAPHITIZATION, AND MEASUREMENT. *Radiocarbon*, 55(2).
- Beer, J., McCracken, K. and Von Steiger, R., 2012. Cosmogenic Radionuclides: Theory and Applications in the Terrestrial and Space Environments. Springer Science & Business Media.
- Bonino, G., Cini Castagnoli, G., Cane, D., Taricco, C. and Bhandari, N., 2001, August. Solar modulation of the galactic cosmic ray spectra since the Maunder minimum. In *International Cosmic Ray Conference* (Vol. 9, p. 3769).
- Carrington, R.C., 1859. Description of a singular appearance seen in the Sun on September 1, 1859. *Monthly Notices of the Royal Astronomical Society*, 20, pp.13-15.
- Cliver, E.W., Feynman, J. and Garrett, H.B., 1990. An estimate of the maximum speed of the solar wind, 1938–1989. *Journal of Geophysical Research: Space Physics*, 95(A10), pp.17103-17112.
- Jackson, A., Jonkers, A.R. and Walker, M.R., 2000. Four centuries of geomagnetic secular variation from historical records. *Philosophical Transactions of the Royal Society of London A: Mathematical, Physical and Engineering Sciences*, 358(1768), pp.957-990.
- Lal, D. and Peters, B., 1967. Cosmic ray produced radioactivity on the earth. In *Kosmische Strahlung II/Cosmic Rays II* (pp. 551-612). Springer Berlin Heidelberg.
2013. Solar storm risk to the north american electric grid.
- Masarik, J. and Beer, J., 1999. Simulation of particle fluxes and cosmogenic nuclide production in the Earth's atmosphere. *Journal of Geophysical Research: Atmospheres*, 104(D10), pp.12099-12111.
- McCracken, K.G., Dreschhoff, G.A.M., Zeller, E.J., Smart, D.F. and Shea, M.A., 2001. Solar cosmic ray events for the period 1561–1994: 1. Identification in polar ice, 1561–1950. *Journal of Geophysical Research: Space Physics*, 106(A10), pp.21585-21598.

- Mekhaldi, F., Muscheler, R., Adolphi, F., Aldahan, A., Beer, J., McConnell, J.R., Possnert, G., Sigl, M., Svensson, A., Synal, H.A. and Welten, K.C., 2015. Multiradionuclide evidence for the solar origin of the cosmic-ray events of AD 774/5 and 993/4. *Nature communications*, 6.
- Miyake, F., Nagaya, K., Masuda, K. and Nakamura, T., 2012. A signature of cosmic-ray increase in AD 774-775 from tree rings in Japan. *Nature*, 486(7402), pp.240-242.
- Nemec, M., Wacker, L., Hajdas, I. and Gaggeler, H., 2010. Alternative methods for cellulose preparation for AMS measurement. *Radiocarbon*, 52(3), pp.1358-1370.
- Odenwald, S.F. and Green, J.L., 2008. Bracing for a solar superstorm. *Scientific american*, 299(2), pp.80-87.
- Odenwald, S.F., 2001. *The 23rd cycle: learning to live with a stormy star*. Columbia University Press.
- Oeschger, H., Siegenthaler, U., Schotterer, U. and Gugelmann, A., 1975. A box diffusion model to study the carbon dioxide exchange in nature. *Tellus*, 27(2), pp.168-192.
- Parker, E.N., 1958. Dynamics of the Interplanetary Gas and Magnetic Fields. *The Astrophysical Journal*, 128, p.664.
- Parker, E.N., 1963. Interplanetary dynamical processes. New York, *Interscience Publishers*, 1963., 1.
- Reames, D.V., 1999. Particle acceleration at the Sun and in the heliosphere. *Space Science Reviews*, 90(3-4), pp.413-491.
- Schweingruber, F.H., 2012. Tree rings: basics and applications of dendrochronology. Springer Science & Business Media.
- Simpson, J.A., 1983. Elemental and isotopic composition of the galactic cosmic rays. *Annual Review of Nuclear and Particle Science*, 33(1), pp.323-382.
- Skog, G., Rundgren, M. and Sköld, P., 2010. Status of the Single Stage AMS machine at Lund University after 4years of operation. Nuclear Instruments and Methods in Physics Research Section B: Beam Interactions with Materials and Atoms, 268(7), pp.895-897.

- Stenström, K., Skog, G., Georgiadou, E., Genberg, J. and Johansson, A., 2011. A guide to radiocarbon units and calculations. *LUNFD6 (NFFR-3111)/1-17/(2011)*.
- Sturm, M. and Lotter, A.F., 1995. Lake sediments as environmental archives. *EA WAG News E*, 38, pp.6-9.
- Stuiver, M. and Braziunas, T.F., 1993. Sun, ocean, climate and atmospheric $^{14}\text{CO}_2$: an evaluation of causal and spectral relationships. *The Holocene*, 3(4), pp.289-305.
- Usoskin, I.G., Solanki, S.K., Kovaltsov, G.A., Beer, J. and Kromer, B., 2006. Solar proton events in cosmogenic isotope data. *Geophysical research letters*, 33(8)
- Wacker, L., Fülöp, R.H., Hajdas, I., Molnár, M. and Rethemeyer, J., 2013. A novel approach to process carbonate samples for radiocarbon measurements with helium carrier gas. *Nuclear Instruments and Methods in Physics Research Section B: Beam Interactions with Materials and Atoms*, 294, pp.214-217.
- Wieler, R., Beer, J. and Leya, I., 2013. The galactic cosmic ray intensity over the past 106–109 years as recorded by cosmogenic nuclides in meteorites and terrestrial samples. *Space Science Reviews*, 176(1-4), pp.351-363.